Proceedings World Geothermal Congress 2015
Melbourne, Australia, 19-25 April 2015

Stibnite Scaling in a Binary Power Plant in Turkey

Baran KAYPAKOĞLU[1], Niyazi AKSOY[2], Umran SERPEN[3], Mehmet ŞİŞMAN[1]

[1]Maren Geothermal Energy Inc, 097000- Germencik-Aydin- Turkey

baransmail@gmail.com

msisman@maren.com.tr

[2]Dokuz Eylul University, Geothermal Energy Research and Application Center 35120 Torbali - Izmir

niyazi.aksoy@deu.edu.tr

[3]NTU Geothermal Energy Consultancy Ltd. 35260 Konak –İzmir –Turkey

umranserpen@ntujeotermal.com.tr

Keywords: Stibnite, scaling, binary plant, Turkey.

ABSTRACT

A geothermal binary cycle power plant in Germencik Turkey has shown a serious decrease in performance at the beginning of summer 2013. Increase in the differential pressure of the power plant suggested that clogging was present in the system. All heat exchanger units were opened and a black-greyish scale with a thickness varying between 1 to 4 mm was encountered in all heat exchangers. Deposits were analyzed and the results showed that they consist of %60-70 antimony and %30-40 sulfide, which led to the conclusion that stibnite was the main cause of scaling in the system. This was the first recorded stibnite scaling phenomenon in Turkey. Power production drop due to stibnite, analysis for antimony and its occurring conditions have been discussed in this paper.

1. INTRODUCTION

Turkey is a country with rich geothermal resources which are used for both district heating and electrical power generation as well as spa centers and greenhouse heating. The country consists of several E-W graben systems created by N-S extension caused by the northward push of the Afro-Arabian Plate. The most productive fields discovered up to now reside in the western part of the country, especially in Büyük Menderes Graben (Serpen et al, 2009).

There are 16 geothermal power plants in Turkey right now (15 in BMG) with a total capacity of 311.871 MW and this capacity is expected to double by the end of 2015. Most of the geothermal fields in Turkey are low to medium enthalpy fields, thus binary power plants are the most preferred machines for electricity generation. Ormat Technologies Inc. leads the binary type plant market by a long shot and is followed by Atlas Copco and TAS Energy Inc.

Geothermal fluid chemistry in the BMG region are all similar, with Na, Cl and HCO_3 being highest in concentration respectively. Chloride content is highest at the west of the graben and decreases due east. CO_2 concentrations are probably the highest in the world, ranging from 0.01 to 0.04 of total mass flow (Aksoy, 2014). This leads to the formation of CO_3 and brings with it the risk of calcite scaling. Phosphonate based inhibitor injection is the common preferred method across the graben for the prevention of calcite scaling.

The first geothermal power plant in Turkey, the Kızıldere power plant, which had started to generate power in 1984 did face serious calcite scaling problems before the introduction of decent (cost-effective) scale inhibitors into the market. Acidizing and mechanical reaming were implemented in certain time intervals which eventually caused loss of money and time (Durak 1995) . Irem power plant is struggling with a different scaling problem right now, comparable to Kızıldere in the same way that there is no inhibitor solution yet developed that will reduce the financial loss due to stops and long-term losses due to decline in the heat transfer rate of the heat exchangers.

1.1 Germencik and Gümüşköy geothermal fields

Germencik geothermal field resides in the western part of BMG, just before the graben changes direction to southwest. The field was discovered by Mineral Research and Exploration (MTA), a governmental institution, in 1968. The first operator Güriş Construction Inc. constructed a 47 MW capacity single flash power plant in cooperation with Mitsubishi Co. In 2011, Maren Energy Inc. invested in the field with a 20 MW binary type Ormat Energy Converter (Irem power plant), followed by two more 24 MW ORC's constructed in 2012. Gümüşköy geothermal field resides in the westernmost of BMG and is occupied by BM holding company which operates two 6.6 MW TAS energy binary type power plants.

There are 7 power plants under construction in Germencik field right now. Güriş Construction Inc. is installing two double flash and three binary type Ormat Energy Converters, all expected to constitute a total capacity 162 MW. Maren Energy Company is installing another 24 MW ORC which is expected to be commissioned by the end of summer 2014.

Figure 1: Büyük Menderes Graben and the locations of installed geothermal power plants on the graben

1.2 Irem power plant

Irem ORC construction started at the beginning of 2011 and the plant was commissioned in December 2011. It is a binary type plant which started its production with 3 production and 4 reinjection wells. Later, one more production and two more reinjection wells were added to operation.

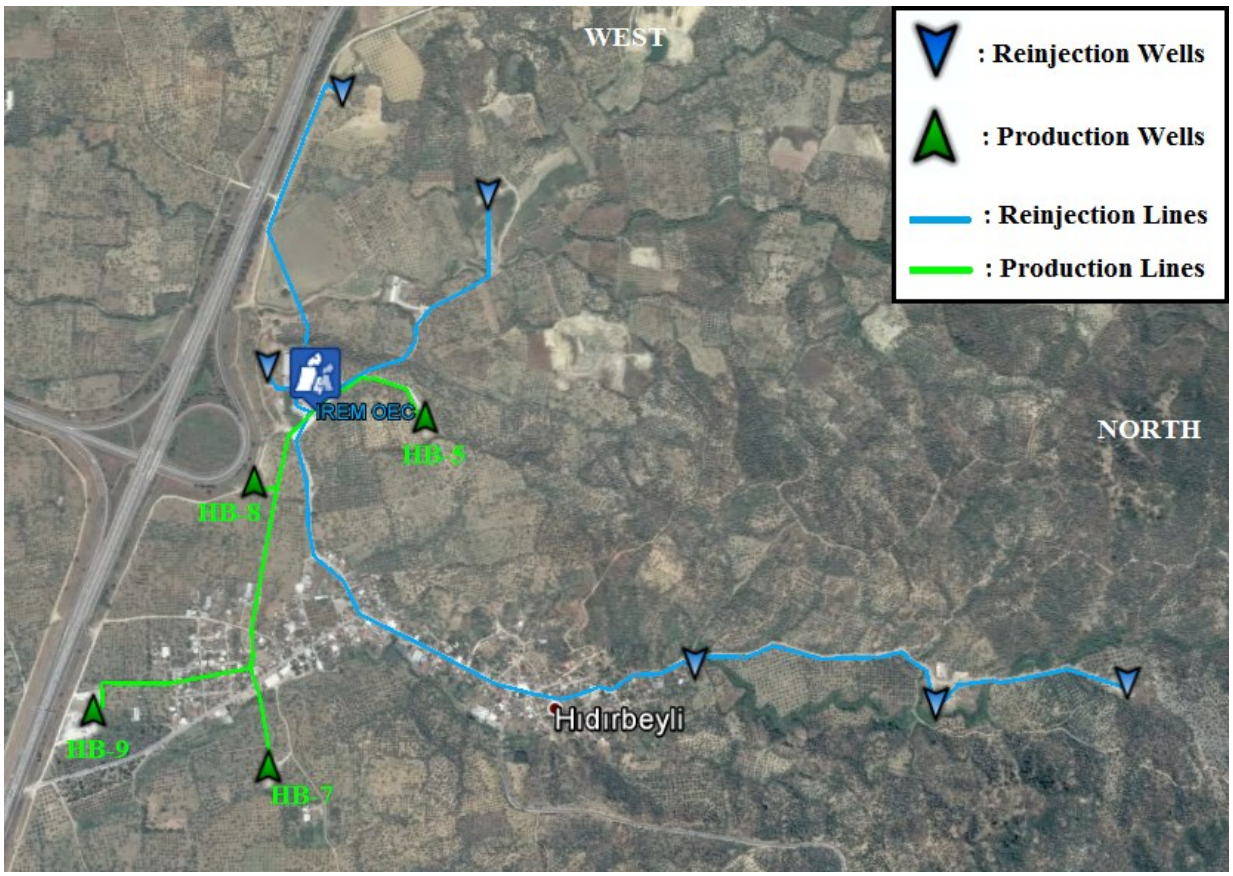

Figure 2: Irem power plant production and reinjection layout.

The plant is designed for 1210 t/h brine at a temperature of 160˚C and is designed to produce 17 MW of gross power at an ambient temperature of 17.5˚C degrees. It runs with an air cooled condenser, thus like all air cooled power plants the production over a year oscillates inversely proportional with ambient temperature.

1.3 Chemistry of brine

All production wells in Irem are Na-Cl-HCO_3 type and their electrical conductivities are about 6000 µmho/cm. There is %2 of non-condensable gases in total mass flow and the NCG consists of 98.89% CO_2 and about 1500 ppm H_2S while there are also traces of nitrogen and methane. Two phase flow coming from the well is separated in a cyclone separator at 8 barg and according to the chemical models done there is about 2000 ppm of CO_2 and 16 ppm of H_2S dissolved in brine after the separation process. Table 1 is a summarization of the chemical content of Irem production wells.

Table 1: Chemical content of Irem production wells

Parameters	HB5, mg/L	HB7, mg/L	HB8, mg/L
pH	6.93	6.91	6.87
Na+	1522	1544	1504
Cl-	1120	1636	1099
HCO3-	1610	1501	1562
SiO2	216	243	238
B	62	67	61
Ca++	24	20	20
K+	103	111	106
As	0.208	0.349	0.185

2. SCALING AND PRODUCTION MONITORING IN IREM POWER PLANT

As said before Irem power plant was commissioned in late 2011. After then, the main vaporizer was opened for mechanical cleaning twice due to calcite scaling in 6 months intervals. Calcite scaling only occurred in the main vaporizer where the temperature of brine is highest and thus the solubility of calcite is lowest. Reinjection temperatures were carefully regulated to prevent silica scaling so no silica scaling was expected nor seen in the preheaters or in the low pressure vaporizer.

Scaling in the plant is tracked by monitoring pressures and calculating the heat duty of the heat exchangers continuously. Differential pressure monitoring is one of the most common methods to monitor clogging in any flow system. The most important differential pressure in Irem ORC was thought to be the first pass (P2-P1) as this section was where the brine had the highest scaling tendency of calcite. But the differential pressure “P3-P2” threw a curve at us by a steep increase at the beginning of summer 2013.

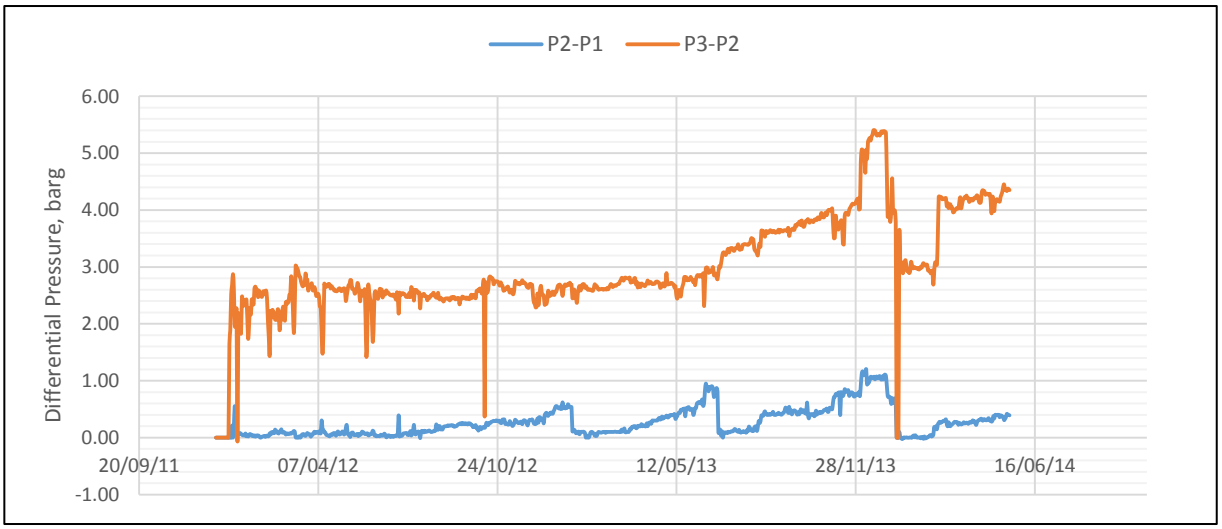

Figure 3: Differential pressures Irem OEC P2-P1 & P3-P2 (refer to figure 8)

In fact a slight increase of 0.1-0.2 barg in P3-P2 is evident after 24/10/12 but this change was overlooked as it was very small.

2.1 Production loss

Production decline in Irem power plant started to show itself in the beginning of summer 2013. Figure 4 is a two years trend of the thermal energy harnessed in the plant versus the ambient temperature. Thermal energy oscillates with ambient temperature until point "1" shown on the figure which corresponds to May 2013. After then a serious decline is seen until the thermal energy drops to about 80 MWt. We can consider a total loss of 30 MWt power until point "2", corresponding to a loss of approximately 4 MWe power produced, taken 0.13 as the thermal efficiency of the plant.

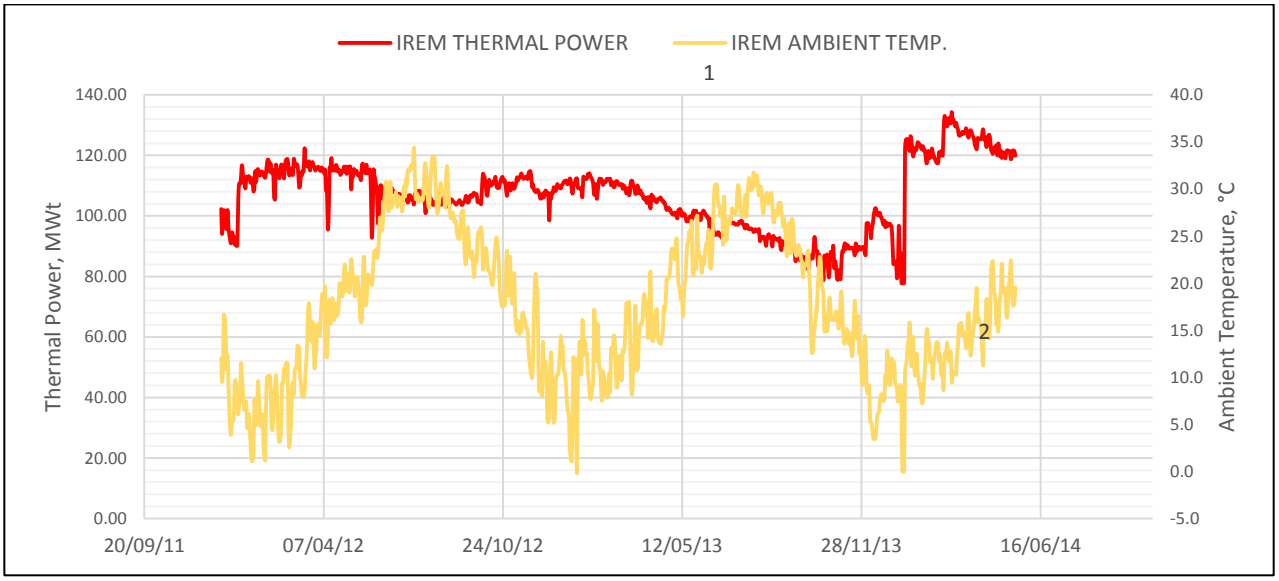

Figure 4: Irem ORC thermal power and ambient temperature

It is evident that the production loss started earlier than point "1" comparing the thermal power for the first two winters in figure 5. Thermal power in the second winter is approximately 10 MWt lower than the first winter.

2.2 Scales encountered in the heat exchangers

Plant shut down and all heat exchangers were opened at the beginning of winter 2014. A black-greyish scale with a thickness varying between 1 to 4 mm was encountered in all heat exchangers. The thickest scales (4-5 mm) were at the third pass of the high pressure vaporizer and at the fourth and fifth passes of the low pressure vaporizer. Scale colors changed towards the preheaters and they became purplish in the first 3 passes of the preheaters and reddish-orange at the last pass. Thickness was about 1-2 mm in preheaters.

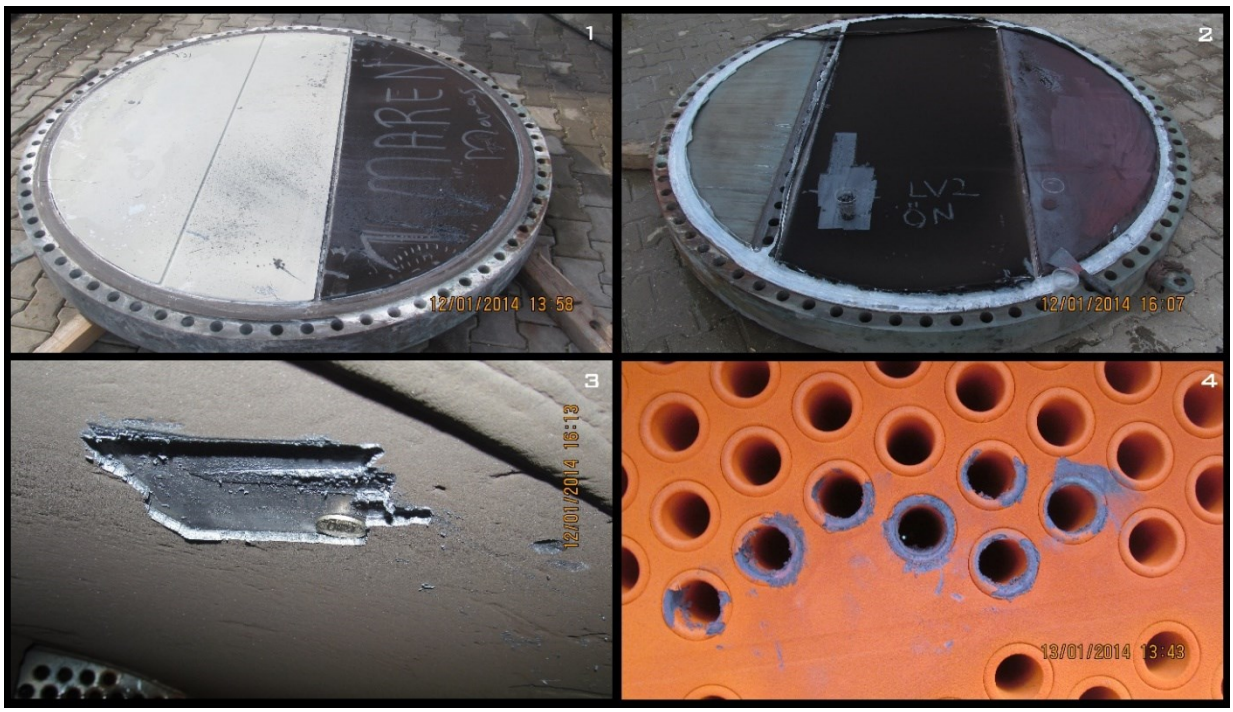

Figure 5: Scales encountered in Irem heat exchangers; 1: HP vaporizer, 2: LP vaporizer, 3: HP&LP vaporizer, 4: preheater last pass

High pressure vaporizer and low pressure vaporizer both consist of three passes for brine while preheaters in both levels have four passes each. Only one preheater is shown in figure 6 as the inlet temperature of brine in both heat exchangers is the same and so are the scaling conditions.

A systematic approach was taken for the analysis of the scales. Each pass of all heat exchangers were numbered and samples were taken accordingly since there were color shifts which could be due to different scales. But surprisingly no matter what the color was the analysis results suggested antimony sulfide for all the samples.

Scale samples were numbered according to the partition where they were taken from. An average scale thickness in each partition was recorded. Figure 7 shows the scale thickness and temperature along the process path.

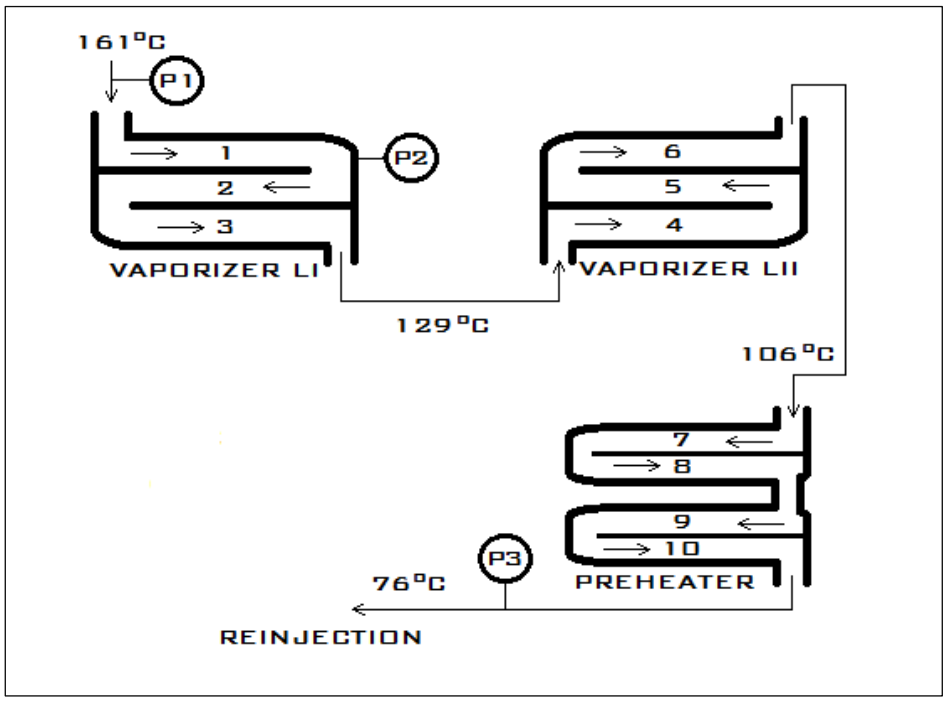

Figure 6: A basic scheme of the brine process cycle and numbering of the heat exchanger partitions.

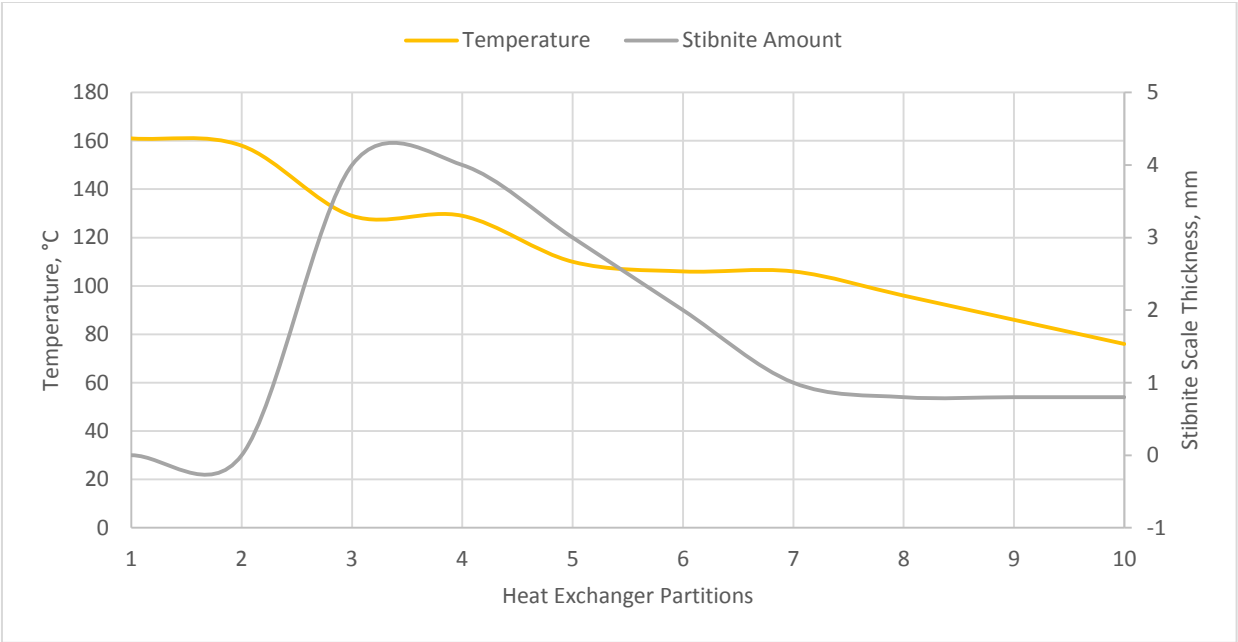

Figure 7: Stibnite precipitation amount along the brine process path in the plant. X axis is the heat exchanger partitions shown in figure 6 above.

Although scales in the preheaters were much thinner than they were in the vaporizers, scales encountered in the preheaters were harder and denser. Antimony orange (amorphous stibnite) that covered the thin hard stibnite scales however were soft like powder.

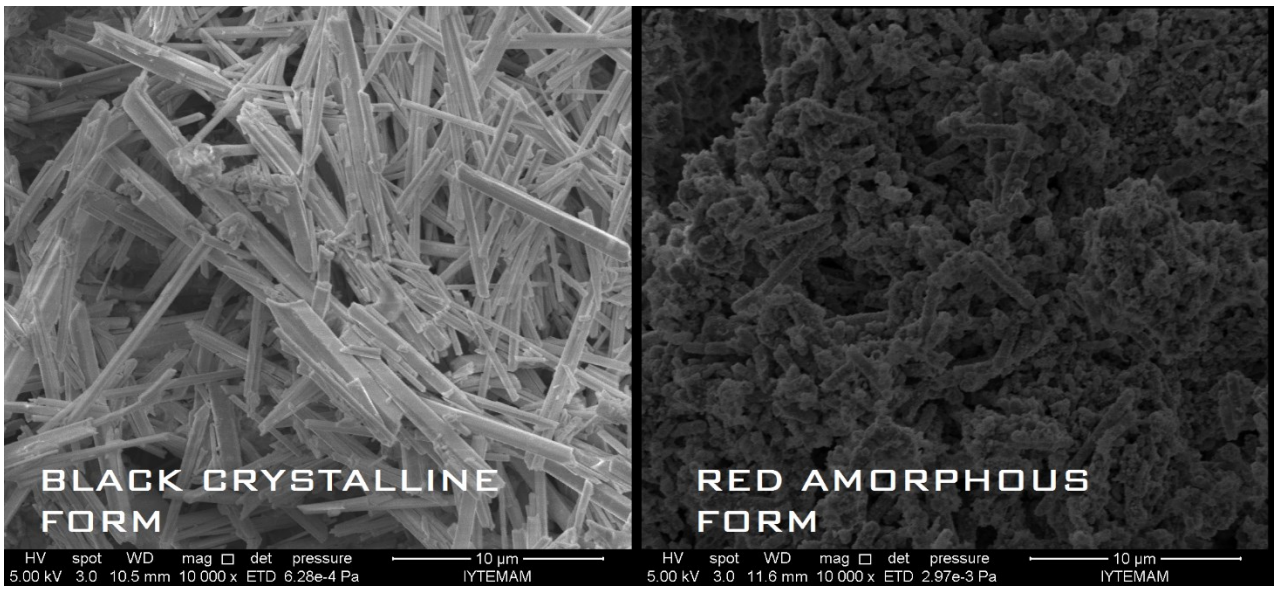

Figure 8: Scanning electron microscope images of black crystalline form and red amorphous form of stibnite.

High pressure water jet cleaning was applied to all heat exchangers and it was harder to clean stibnite compared to calcite according to the staff that did the cleaning. The heat duty of the preheaters increased about 5 MW while the increase was about 15 MW for the high pressure vaporizer and 10 MW for the low pressure vaporizer.

2.3 Antimony in the environment and geothermal industry

Antimony is present in the environment in the mineral form stibnite, the chemical formula of which is Sb_2S_3. Concentration of antimony in the earth's crust is about 0.2-0.3 ppm. In unpolluted natural waters concentrations of dissolved antimony are less than 1 µg/l, but concentrations can reach up to 100 times due to anthropogenic sources (Filella, 2001).

Antimony trisulfide exists as a black crystalline solid and as an amorphous red-orange powder. The mixtures can also make some colors in between such as carmine or brownish red. The mineral has several synonyms some of which are; grey antimony, antimony orange, antimony sulfide and antimony vermilion. It is very slightly soluble in water (175 µg/0.1 liter) and more soluble in alkalies, concentrated hydrochloric acid, sulfide solutions and in ethanol (Herbst, 1985; Lewis, 2002; Lide, 2001; Merck, 2001).

Stibnite scaling phenomenon in geothermal industry was only recorded in New Zealand, Italy, Berlin and El Salvador up to now (Wilson, 2007). One reason for scarcity in publications about stibnite precipitation in geothermal industry could be the low quantity of binary type power plants in the past. With the increase of binary type plant utilizations all over the world it is expected to encounter higher number of stibnite phenomenon in geothermal industry as binary type plants provide suitable conditions for stibnite precipitation due to high temperature drops in the process.

2.4 Brine analysis for antimony

After mechanical cleaning brine samples were taken from all production wells and from the inlet and outlet of the OEC for antimony analysis and to conduct mass balance calculations in order to predict the scaling amount. One set of samples were taken with no preservation while the other set of samples were preserved with alkali. All samples are taken with cooling coils to prevent flashing. Table 2 shows the results.

Looking at table 2, there is either an inaccuracy in the analysis, or additional antimony is being carried from the pipelines or equipment to the plant inlet. A study by Keny (2014) writes about antimony traces coming into the pressurized heavy water reactors in a nuclear plant from the pump seals and bearings that contain antimony-impregnated graphite. Bearing such a possibility in mind this issue should further be investigated.

Focusing on the precipitation amount of antimony in the plant, calculations according to the results for non-preserved samples suggest 5.8 kg of antimony precipitation while calculations for samples preserved with alkali suggest 12.7 kg of scaling per day. Pilot studies show better recovery of antimony in samples preserved by alkali since antimony solubility increases with increasing pH (Wilson, 2007). Therefore 12.7 kg of precipitation per day seems more likely, but further brine analysis should be conducted, preferably with a different laboratory to have a more clear answer.

Table 2: Antimony analysis for mass balance calculations

Sampling Method	Parameters	HB5, mg/L	HB7, mg/L	HB8, mg/L	Plant inlet, mg/L	Reinjection , mg/L
NEUTRAL SAMPLES (NOT TREATED)	pH	7.1	7	7.1	7.3	7
	Antimony	0.3	0.3	0.3	0.4	0.2
	Arsenic	0.1	0.3	0.1	0.2	0.2
ADDITION of CAUSTIC,ph >12	pH	12	11.7	11.9	12	11.4
	Antimony	0.2	0.43	0.31	0.57	0.13
	Arsenic	0.1	0.32	0.17	0.22	0.098

2.5 Solubility of stibnite in water

Stibnite dissolves in water according to the following equation:

$$Sb_2S_3 + 6H_2O = 2Sb(OH)_3 + 3H_2S \quad (1)$$

Antimony hydroxide dissociates to form free hydrogen ions and $H_2SbO_3^-$ anion. The degree of this dissociation increases with increasing pH, so does the solubility of stibnite (Brown, 2011).

Equilibrium equation above also suggests that increased concentrations of hydrogen sulfide increases the amount of stibnite precipitation. Below is the solubility equation created with the data presented in Zotov et al.,(2003) which explains the dependence of stibnite solubility on temperature (Wilson, 2007).

$$\text{Log } K = -7640.3/T + 7.213 \quad (2)$$

To sum up, stibnite solubility increases with temperature and pH while it decreases with increasing H_2S concentration.

3. FUTURE CONCERN

The first and the only stibnite scaling phenomenon in Turkey is recorded. However this phenomenon is expected to increase in the near future as binary type power plant utilizations are on a serious rise in Turkey. There is yet no chemical inhibitor developed to prevent stibnite scaling. Chemical companies should start their research and development on this issue as soon as possible as stibnite scaling prevention will be an important determinant for customers having this problem.

Since pH is one of the most important factors affecting stibnite solubility, it may be possible to prevent this scaling by increasing the pH of the brine. However this is not a realistic solution as it will cause carbonates to precipitate.

Cleaning with high pressure water jet is time consuming and messy, but it usually is the only option. The most important matter to be decided is the time. One should not wait until differential pressures reach serious levels, because decline in heat transfer starts much before recognizable increases in differential pressure.

Chemical cleaning such as re-circulation with caustic soda can be a solution to dissolve stibnite and clean the tubes. However caustic may be corrosive and can cause serious damage to carbon steel. Thus this method needs to be implemented very carefully in order to avoid long term damages.

REFERENCES

Aksoy, N. (2014) Power generation from geothermal resources in Turkey. *Renewable Energy* **68,**595-601

Brown, K. (2014) Antimony and arsenic sulfide scaling in geothermal binary plants. *Proceedings International Workshop on Mineral Scaling.*

Durak, S., Erkan, B. And Aksoy, N. (1995): Calcite removal from wellbores at Kızıldere geothermal field, Turkey. *Proceedings: 15th Geothermal Workshop*, Auckland, New Zealand.

Filella, M., Belzile, N., Chen, Yu-Wei. (2002) Antimony in the environment: a review of focused on natural waters I. Occurrence. Earth-Science Reviews 57, 125-176.

Herbst, K.A., Rose, G., Hanusch, K., Schumann, H.& Wolf, H.U. (1985) Antimony and antimony compounds. In: Elvers, B., Hawkins, S. & Russey, W., eds., *Ullmann's Encyclopedia of Industrial Chemistry,* Vol. A3, VCH Publishers, pp 55-76

Lewis, R.J.,ed. (2002) *Hawley's Condensed Chemical Dictionary,* 14thed. (On CD-Rom). NY, John Wiley & Sons Inc.

Lide, D.R., ed. (2001) *CRC Handbook of Chemistry and Physics,* 80th ed. (On CD-Rom) Boca Raton, FL, CRC Press

Merck (2001) Antimony trisulfide. *The Merck Index,* 12.3 ed. (On CD-Rom). Boca Raton, FL, Chapman & Hall. [Monograph Number 719]

Keny, S.J., Kumbhar, A.G., Sanjukta, A., Pandey, S., Ramanathan, S., Venkateswaran, G. (2014) Antimony sorption and removal on carbon steel/magnetite surfaces in relation to pressurized heavy water reactors. *Current Science,* Vol.106, No.8.

Serpen, U., Aksoy, N., Ongur, T. and Korkmaz, E. D. (2008): Geothermal energy in Turkey: 2008 Update. *Geothermics* **38**, (2009) 227–237.

Wilson, N, Webster-Brown, J., Brown, K.L. (2007) Controls on stibnite precipitation at two New Zealand geothermal power stations. *Geothermics,* 36, 330-347

Zotov, A.V., Shikina, N.D., Akinfiev, N.N., (2003) Thermodynamic properties of the Sb(III) hydroxide complex $Sb(OH)_{3(aq)}$ at hydrothermal conditions. Geochim. Cosmochim. Acta 67, 1821-1836.